Stably Stratified Atmospheric Boundary Layers

L. Mahrt

NorthWest Research Associates, Redmond, Washington 98052, and College of Earth, Ocean, and Atmosphere, Oregon State University, Corvallis, Oregon 97331; email: mahrt@nwra.com

Annu. Rev. Fluid Mech. 2014. 46:23–45

First published online as a Review in Advance on July 29, 2013

The *Annual Review of Fluid Mechanics* is online at fluid.annualreviews.org

This article's doi: 10.1146/annurev-fluid-010313-141354

Keywords

stratified turbulence, nocturnal boundary layer, submeso motions, gravity waves, atmospheric turbulence

Abstract

Atmospheric boundary layers with weak stratification are relatively well described by similarity theory and numerical models for stationary horizontally homogeneous conditions. With common strong stratification, similarity theory becomes unreliable. The turbulence structure and interactions with the mean flow and small-scale nonturbulent motions assume a variety of scenarios. The turbulence is intermittent and may no longer fully satisfy the usual conditions for the definition of turbulence. Nonturbulent motions include wave-like motions and solitary modes, two-dimensional vortical modes, microfronts, intermittent drainage flows, and a host of more complex structures. The main source of turbulence may not be at the surface, but rather may result from shear above the surface inversion. The turbulence is typically not in equilibrium with the nonturbulent motions, sometimes preventing the formation of an inertial subrange. New observational and analysis techniques are expected to advance our understanding of the very stable boundary layer.

1. INTRODUCTION

Two-dimensional modes: primarily horizontal motions in the strongly stratified boundary layer with negligible vertical motion and minimal vertical coherence, but often with significant vertical vorticity

Classical understanding of stably stratified atmospheric boundary layers is well described in a number of textbooks (Garratt 1992, Panofsky & Dutton 1984, Sorbjan 1989, Stull 1988, Wyngaard 2010). Numerous studies in the past decade have examined the behavior of turbulence in very stable boundary layers not described by classical concepts. Fundamental features of the common very stable boundary layer still remain a mystery.

Stable boundary layers can be generated by the advection of warm air over a colder surface, as in the flow of warm air from land over colder coastal waters (Smedman et al. 1993). However, radiative cooling of the ground surface, as occurs with nocturnal conditions under relatively clear skies, is the most common source of stable boundary layers. The net radiative cooling of the ground/vegetation surface induces a vertical temperature gradient in the atmosphere and the transfer of heat from the atmosphere to the cooler surface. This heat loss to the ground surface cools the adjacent air with attendant formation of a stably stratified inversion layer. Such cooling is greatest with completely clear skies, small water vapor content, and small contaminant concentration. These conditions result in small downward radiation to the surface and thus large net radiative cooling of the surface. Dry soil conditions reduce the thermal conductivity of the soil and thus reduce the upward soil heat flux. Less upward heat flux in the soil leads to greater cooling of the ground surface. This process may begin an hour or two before sunset when the incoming solar radiation first becomes less than the net long-wave radiative cooling. Stable boundary layers may survive for several hours after sunrise and can survive the entire day with low–winter sun angles, particularly in valleys and basins.

Turbulence in stratified flows in laboratory settings and numerical simulations is easier (but still difficult) to understand (Ohya et al. 2008, Riley & Lelong 2000). With numerical modeling and laboratory studies, the lower boundary is flat and homogeneous, the imposed external forcing is stationary, and disturbances do not propagate from outside the domain. Riley & Lindborg (2008) offered some specific applications of laboratory and numerical results to geophysical flows. The extensive review of turbulence in strongly stratified flows by Hopfinger (1987) details aspects of turbulence decay and coexistence with internal waves and horizontal two-dimensional modes for a variety of flow configurations. Two-dimensional, or quasi-horizontal, modes are not significantly coupled in the vertical direction and develop vertical shear until such shear leads to the instability and breakdown of the mode.

Fernando & Weil (2010) have surveyed some of the complexities of atmospheric stable boundary layers. Atmospheric boundary layers are complicated by nonturbulent motions occurring simultaneously on a variety of scales, the possible importance of radiative flux divergence of the air within the boundary layer, surface condensation, and variable cloudiness. Many data for complex conditions in the stable boundary layer are excluded from the analyses reported in the literature. Such exclusions often involve restrictions on nonstationarity or conditions on the minimum allowed value of the turbulence energy.

An examination of turbulence first requires a working definition of turbulence. Tennekes & Lumley (1972) provided a detailed group of requirements for turbulence. Busch et al. (1969) offered a simplified definition of turbulence that requires vorticity distributed randomly in time and space, dissipation and diffusion to a higher degree than can be accounted for by the molecular diffusivities and the mean strain rate, and energy transferred from larger scales to smaller scales through a continuous cascade process in wave-number space.

The energy cascade argument is partly based on spectral decompositions. The spectra depend on whether the information originates as a time series at a fixed point or as spatial observations at a fixed time. The spectra also depend on the basis set of the decomposition (Mahrt & Howell 1994),

such as global Fourier sine functions and various local wavelet basis sets. The energy cascade may not be completely continuous because of short-circuiting of the spectrum. For example, thin zones of large shears can develop within large eddies, followed by instabilities and the direct generation of fine-scale structure (Hunt & Vassilicos 1991, Vassilicos & Hunt 1978), without significant involvement of intermediate-scale eddies. The formation of sharp shear zones can result from vortex stretching by large eddies (Gerz et al. 1994), which then break down directly into fine-scale eddies. Short-circuiting of canopy turbulence is discussed in Finnigan (2000).

Intermittency: strong variability of the turbulence in space and time

For very stable conditions, the definition of turbulence might be further relaxed to allow for extreme intermittency and strongly skewed probability distributions of turbulence quantities corresponding to infrequent mixing events. With increasing stability, the characteristics of traditionally defined turbulence are more difficult to identify. Virtually all turbulence quantities estimated from observations are based on Reynolds averaging, as in the papers cited in this review. At the same time, we recognize difficulties in interpreting such averaging (McNaughton 2012).

This review only briefly summarizes the classical formulations of the stably stratified boundary layer and then emphasizes frequent situations in which such formulations are not valid. As a result, this review focuses on observations, and the reader is referred to the textbooks cited above for an introduction to modeling approaches. Even then, numerous useful observational references are omitted, and the enthusiastic reader must explore the references within the papers cited here. I do not consider the residual layer above the stable boundary layer (Tjernström et al. 2009), low-level jets (Andreas et al. 2000, Banta et al. 2006, van de Wiel et al. 2010), surface heterogeneity, variable cloudiness (Cava et al. 2004), surface fog formation (Duynkerke 1999), the role of the soil and vegetation, or the surface energy budget. Below I begin with a quick look at traditional similarity theory.

2. SIMILARITY THEORY

The atmospheric boundary layer is vertically partitioned into the roughness sublayer, the overlying surface layer, the outer layer or main planetary boundary layer, and a transition or entrainment layer, as illustrated in **Figure 1*a***. These idealized layers are most applicable to weakly stable conditions (Section 3) and are inapplicable to very stable conditions (Section 4). In the roughness sublayer, the flow is influenced by individual vegetation elements (Finnigan 2000, Katul et al. 1999), and similarity theory for the roughness sublayer is not widely used.

2.1. Surface Layer

The surface layer is normally expressed in terms of Monin-Obukhov similarity theory, which is applied in most atmospheric models. The flux-gradient relationship for an arbitrary variable F for this theory is expressed in terms of nondimensional gradients

$$\phi_F \equiv \frac{\kappa z \partial \bar{F}/\partial z}{F_*}, \tag{1}$$

where the overbar denotes time averaging. For the along-wind momentum, $\bar{F} = \bar{u}$ and $F_* = u_*$, where u_* is the square root of the surface momentum flux. For heat, $\bar{F} = \bar{\theta}$ and $F_* = -\theta_* \equiv \overline{w'\theta'}/u_*$, where $\overline{w'\theta'}$ is the surface heat flux. Once computed, turbulent quantities are often averaged over a longer time period to reduce random errors, provided that the turbulence is relatively stationary.

The nondimensional gradient is formulated as a function of stability

$$\phi_F = f(z/L), \tag{2}$$

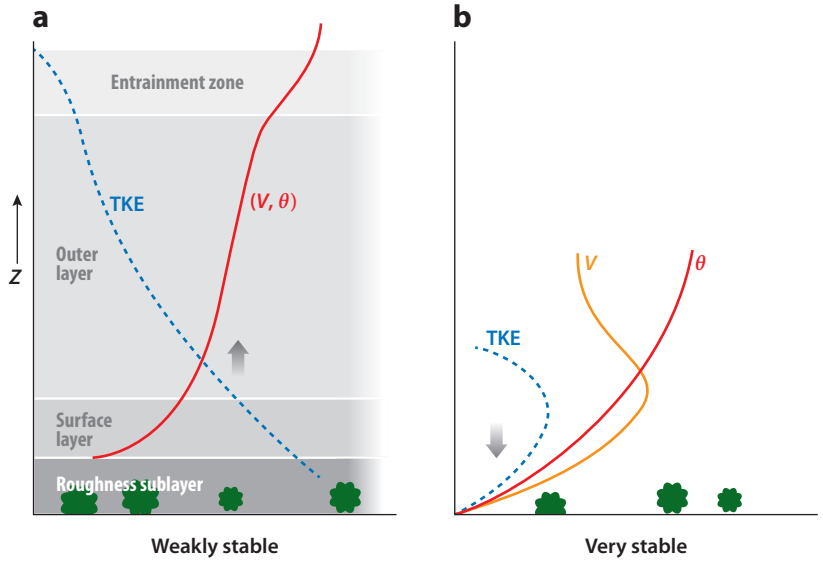

Figure 1

A greatly simplified division of boundary layers into (*a*) the weakly stable regime and (*b*) the strongly stable regime. (*a*) Plausible vertical structure corresponding to the relatively well-defined weakly stable regime. The gray zones delineate idealized horizontal layers. The entrainment zone is definable only for the weakest stability. The dashed blue curve depicts the typical height dependence of the turbulence energy (TKE). The solid red line represents the general structure of both the potential temperature, θ, and the wind speed, V. The gradient arrow indicates the usual direction of the vertical transport of turbulence energy. (*b*) One of numerous different vertical structures for the very stable boundary layer. The red solid curve represents the potential temperature, and the orange solid curve represents the wind speed for the case of a near-surface wind maximum. For very stable conditions, various vertical structures are possible, and the vertical structure is generally nonstationary. In reality, the very stable boundary layer is typically an order of magnitude thinner than the weakly stable boundary layer.

where $f\,(z/L)$ is the stability function, and L is the Obukhov length $\equiv u_*^3\bar{\theta}/(\kappa g\overline{w'\theta'})$, where κ is the von Kármán constant and g is the acceleration of gravity. The stability function accounts for the decrease of turbulence strength with increasing stability due to the increasing buoyancy destruction of turbulence. With greater stability (large z/L), the flux is smaller for a given vertical gradient.

Similarity theory often contains shared variables on both sides of the equation, which can lead to self-correlation (Baas et al. 2006, Hicks 1978, Klipp & Mahrt 2004). When the self-correlation is the same sign as the expected physical correlation, as occurs with stable stratification, the physical interpretation of the results becomes ambiguous. For example, both sides of Equation 1 are a function of u_*. With increasing stability, u_* becomes, percentage-wise, more variable than the other variables and eventually dominates the variations on each side, in which case Equation 2 degenerates toward a relationship of u_* to u_*. Anderson (2009) circumvented the influence of self-correlation by fitting relationships between individual variables and then substituting these relationships into the ratios of interest.

From a more general point of view, similarity theory relates turbulence variables to the turbulence itself. The value of similarity theory lies in closing a set of equations by providing an additional relationship. Self-correlation in the stable boundary layer can be reduced using gradient-based

similarity theory (Sorbjan 2010) in which the stability parameter is the gradient Richardson number. With this approach, the turbulence is exclusively related to the mean flow.

2.2. Outer Layer

Similarity theories for the vertical structure of the boundary-layer flow above the surface layer are summarized by Sorbjan (1989) and Garratt (1992). These theories require equilibrium between the turbulence and the boundary-layer depth and use information on the Coriolis parameter. Such theory is matched with surface layer similarity theory to form resistance laws (Sorbjan 1989). For polar nights with no diurnal variation, the structure might be well described by Ekman theory (Grachev et al. 2005). The Ekman profile contains an inflection point that can lead to instability and the growth of longitudinal vortices (Brown 1972). Ekman dynamics also contribute to the diurnally varying boundary layer in midlatitudes but may require modification because of baroclinity (Foster & Levy 1998). With common formation of low-level nocturnal jets, the profile of wind speed in the outer layer between the top of the surface layer and the wind maximum is often approximately linear (Banta et al. 2006).

2.3. Spectral Similarity

The scale dependence of the turbulence is often expressed in terms of Kolmogorov similarity theory, which describes the transfer of energy from the main energy-containing eddies to the fine-scale structure in which kinetic energy is dissipated by viscosity (Tennekes & Lumley 1972). This similarity theory is normally expressed in terms of a Fourier expansion, although such expansions are somewhat ambiguous for turbulence (Tennekes 1976). Such spectral arguments have been extended to lower frequencies to include nonturbulent motions such as gravity waves (Weinstock 1985). Riley & Lindborg (2008) found that the physical interpretation of spectra can be misleading. Different physics can produce similar spectral slopes.

3. BOUNDARY-LAYER REGIMES

Any attempts to classify stable boundary layers will be incomplete or unwieldy because stable boundary layers are influenced by a number of independent forcings, including circulations on a variety of timescales and space scales, net radiative cooling, temperature advection, surface roughness, and surface heterogeneity. The characteristics of the fluctuating flow also depend on the height above the surface. Furthermore, timescale dependence may differ from horizontal-scale dependence, as some motions can propagate at speeds and in directions that are much different from that of the wind vector. **Figure 2** preliminarily defines motions on different scales that are refined in the discussions below. Energy can continuously transfer to smaller scales through a sequence of instabilities or can transfer directly to fine scales (short-circuiting) through the direct shear generation of small-scale turbulence. For example, larger-scale waves can directly generate turbulence by enhancing the shear. The return influence of turbulence mixing and drag on the larger-scale motions is not included in the figure.

In spite of the above complexities, numerous classification schemes for different types of stable boundary layers have been offered. Here we choose a simple scheme that is incomplete but useful for describing the most fundamental changes with increasing stability. The weakly stable regime usually includes a well-defined boundary layer in which the turbulence decreases with height and becomes small at the top of the boundary layer (**Figure 1**). The turbulence is relatively continuous in both time and space. Weakly stable conditions occur with either cloud cover or

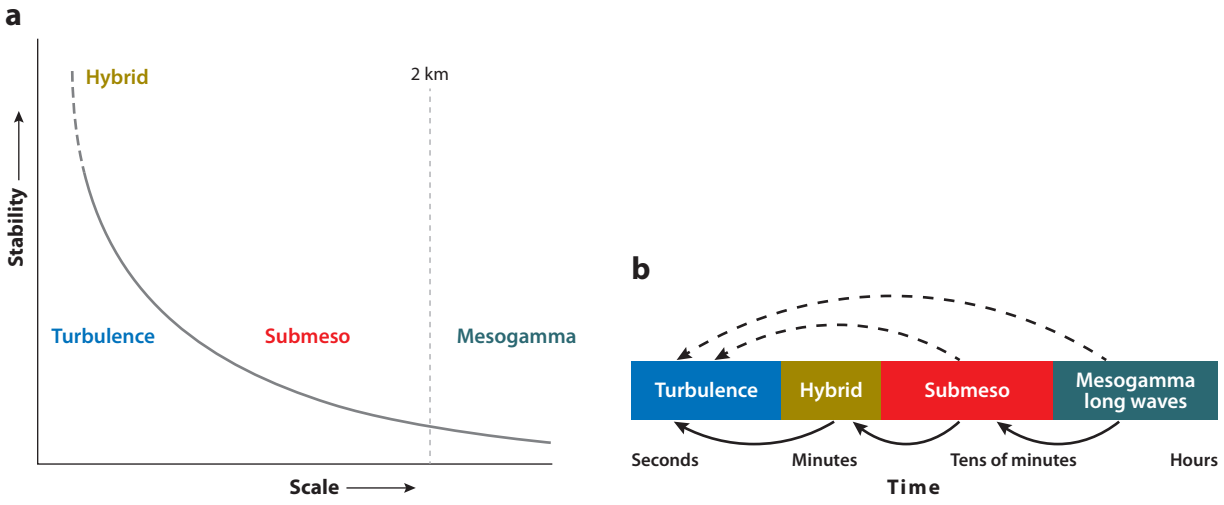

Figure 2

(*a*) The basic regimes in stability-scale space. (*b*) Downscale energy flow (*solid arrows*) in which the *x* axis refers to timescales for observations at a fixed point. The dashed arrows represent short-circuiting of the energy flow directly from larger scales to the turbulent scales. Submeso motions include short gravity waves and a rich variety of other common motion types (see Section 5). Actual motions in the stratified atmospheric boundary layer are often more complex than those accommodated by this simple classification. Flow characteristics can sometimes vary only gradually with scale.

significant airflow. Excluding nonstationarity and heterogeneity, weakly stable regimes generally follow similarity theory and the concepts discussed in Section 2.

The very stable regime occurs with strong stratification and weak winds and does not follow the traditional concept of a boundary layer. For example, the turbulence may increase with height, as sketched in **Figure 1**, and reach a maximum in a layer only intermittently coupled to the surface. The very stable regime will include a variety of different scenarios and vertical structures, and a unifying conceptual picture is not available.

More sophisticated classification schemes may include a transition regime between the weakly stable and very stable regimes. The extremely stable part of the very stable regime, or the radiation regime, can be separated from the very stable regime as a new regime. In the radiation regime, the turbulent heat flux is so weak that the net radiative cooling is balanced primarily by the upward heat flux from the soil (van de Wiel et al. 2003). Then the boundary layer becomes sensitive to soil properties that control the upward heat flux from the soil, such as soil moisture content and thermoconductivity. Extremely stable conditions can also be identified with stability class 5 from Basu et al. (2006) and with the most stable conditions in Grachev et al. (2005) and Sorbjan (2010). The above regimes can be summarized as the weakly stable, transition, very stable, and extremely stable/radiation regimes. In parallel to this classification scheme, the near-calm regime is defined in terms of mean wind speeds that are so weak that the airflow is controlled more by gravity waves and other submeso motions (see Section 5). The near-calm regime includes much of the very stable and extremely stable regimes but also includes cloudy, very weak winds within the weakly stable regime. Classification into different regimes does not recognize all the complexities of the stable boundary layer. We simply partition the boundary layers into a weakly stable regime and a very stable regime.

The separation between the weakly stable and very stable regimes can be defined in terms of a transitional Richardson number. The turbulence decreases with increasing Richardson number

until the Richardson number reaches a transition value, and then varies slowly or not at all with a further increase of the Richardson number (Mahrt et al. 2012). For very stable conditions, the weak dependence on the Richardson number may be related to a relatively weak dependence on the wind speed and near independence from the stratification (Sun et al. 2012). Sun et al. (2012) found that the turbulence increases only slowly with increasing wind speed until the wind speed reaches a threshold value, and then increases more significantly with further increase of the wind speed. Because the wind speed and Richardson number are strongly correlated for very stable conditions, this threshold seems to correspond to the transition between very stable and weakly stable conditions. Intermittency between very weak and significant turbulence occurs when the wind accelerates and decelerates across this threshold value. This threshold value increases with height (Sun et al. 2012) and decreases with surface roughness (Mahrt et al. 2013). Van de Wiel et al. (2012b) posed this threshold in terms of a minimum wind speed needed to maintain continuous turbulence.

4. TURBULENCE IN THE VERY STABLE REGIME

Very stable conditions can be common, even dominant, during seasons with generally fair skies and weak pressure gradients. Very stable conditions can be particularly frequent in basins, local depressions, and valleys with weak downvalley slopes. We now examine this regime in some detail.

4.1. Scale Dependence

The range of turbulence scales decreases with increasing stability, as sketched in **Figure 2*a***. With strong stability, the eddies may become sufficiently confined to small scales that they do not directly interact with the ground surface; this condition is sometimes referred to as z-less stratification. The general applicability of z-less similarity theory was questioned by Grachev et al. (2005).

For very stable conditions, separation between turbulence and waves may not be possible, and an intermediate range of scales appears to have characteristics between those of turbulence and nonturbulent motions. Therefore, there is an additional category in **Figure 2** called hybrid motions. In addition to modes with intermediate characteristics, this category could also include the superposition of turbulent and nonturbulent modes that overlap in timescale. Mahrt et al. (2012) identified hybrid motions with relatively flat circulations (very weak vertical motions) yet with significant downward heat flux due to large coherent temperature fluctuations on the hybrid scale. However, the authors were unable to provide a sharp definition of the hybrid regime because the characteristics seem to vary gradually with scale.

In the atmospheric literature, the term submeso (**Figure 2**) is defined with a variety of different but related criteria. Here, submeso motions (Section 5) refer to any nonturbulent motions on scales smaller than 2 km, the smallest allowed mesogamma scale, as included in **Figure 2** (see the sidebar, Submeso Motions). Unfortunately, one-to-one mapping between the usual time domain of the observations and the space domain is not possible.

4.2. Turbulence Characteristics

The turbulence and mean vertical structure in the very stable regime are quite different from those in the weakly stable regime and are not well described by similarity theory. Deviations from similarity theory and from classical thinking include the following characteristics.

Compared to fully developed turbulence in the weakly stable regime, the turbulent motions in the very stable regime are characterized by (*a*) very small correlations between vertical velocity

SUBMESO MOTIONS

The literature defines the term submeso in various ways and with different terminology, the most common being submeso and submesoscale. Submeso generally includes the complex mix of motions on scales between the main turbulent eddies and smallest mesoscale motions, traditionally specified to be 2 km horizontal scale. The submeso range is defined to extend to larger scales in oceanic studies. Unfortunately, most analyses are carried out in the time domain, and motions on this scale do not adhere to a definite relationship between timescales and horizontal scales. Early uses of the term submeso in the atmospheric literature include urban applications, as in Mestayer & Anquetin (1995). The model SUBMESO has been used to study the formation of cold pools in deep valleys (Anquetin et al. 1998). Submeso motions were allowed to be nonhydrostatic and violate incompressible mass continuity. The direct effect of the Coriolis term on submeso motions is neglected. In the recent literature and the current review, the term submeso is not physically based but rather includes all motions on scales smaller than roughly 2 km that are nonturbulent and is most commonly applied to the stable boundary layer.

fluctuations and scalars (Mahrt et al. 2012); (*b*) predominantly horizontal motions with weak vertical velocity fluctuations and constrained vortex stretching; and (*c*) relatively large temperature fluctuations, which can be posed in terms of exchanges between available potential and kinetic energy (Winters et al. 1995).

The turbulence energy often increases with height and reaches a maximum above the surface inversion layer, referred to as the upside-down boundary layer (Balsley et al. 2006, Mahrt & Vickers 2002). The vertical transport of turbulence energy is downward toward the surface. In such cases, the surface stress may no longer be a relevant scaling variable for the boundary layer (Grachev et al. 2005, Sorbjan 2010). If definable, the boundary layer can be quite thin, less than 10 m deep (Smedman 1988).

Additionally, the inertial subrange may not be detectable in Fourier spectra, pointing to the failure of Kolmogorov similarity theory, or perhaps failure to observe sufficiently small scales (Grachev et al. 2013). Moreover, probability distributions of turbulence quantities change from approximately Gaussian to strongly skewed toward positive values, which is caused by occasional mixing events superimposed on the pervasive background fine-scale turbulence (Mahrt et al. 2012).

With sufficiently weak large-scale flow, the nonturbulent flow comprises primarily nonstationary submeso motions (see Section 5) on scales from meters to several kilometers such that the turbulence cannot maintain equilibrium with the constantly changing speed and direction of the mean flow. The turbulence adjustment timescale is expected to be of order L/u_* (Flores & Riley 2011). The turbulence cannot maintain equilibrium with submeso motions whose timescale is not large compared to the turbulent adjustment timescale. Such nonstationarity contributes to the intermittency of the turbulence (see Section 4.4).

The main transporting eddies, even close to the ground, may be sufficiently small that they do not interact directly with the ground surface (Sun et al. 2012). These eddies may be too small to be adequately sampled with sonic anemometers whose path length is usually approximately 15 cm. Even in the presence of larger eddies that interact with the ground, a significant fraction of the vertical flux may be carried by fine-scale eddies.

In extremely stable conditions, the depth of the boundary layer, if definable, may not be large compared to the height of the roughness elements. In fact, the surface-based boundary layer may be thinner than the height of the roughness elements. For example, in **Figure 3**, the depth of the inferred surface-based boundary layer is of the order of 1 m and is much thinner than the

Figure 3

Observations of striated fog and a thin saturated boundary layer at the surface, commonly observed at this site near Corvallis, Oregon.

height of the trees in the background. More significant turbulence forms independently above the trees. In general, strong stratification can seriously reduce mixing between the vegetation layer and the overlying flow, reducing the effective surface roughness length (Zilitinkevich et al. 2008). Sorting out this influence from possible deviant behavior of the stability function (Equation 2) is not possible with existing observations.

Radiative flux divergence may become important particularly in thin layers close to the surface (Duynkerke 1999, Mukund et al. 2013), although observations of the radiative flux divergence can be subject to large errors (Burns et al. 2003) and are often supplemented or replaced with radiative models.

The very stable boundary layer can often be partitioned in terms of a few layers (Smedman 1988), or semidetached layers bounded by thin zones of strong stratification (Balsley et al. 2003). The formation of thin mixing layers seems to be less common in the atmospheric boundary layer compared to the stratified ocean, although this perception could be related to the better availability of extensive detailed vertical profiling in the ocean. **Figure 3** shows striations of fog, suggestive of layered fine-scale mixing in the atmospheric boundary layer. With strong stratification, horizontal diffusion more effectively transfers material than does vertical diffusion (Sukorianski & Galperin 2013).

4.3. Turbulence at Large Richardson Numbers

The maintenance of turbulence at large Richardson numbers and the lack of a critical Richardson number have been discussed in detail by Galperin et al. (2007) and Sukorianski & Galperin (2013). Turbulence at high Richardson numbers has been noted in numerous atmospheric observational studies (for recent examples, see Yagüe et al. 2006, Luhar et al. 2009). The generation and maintenance of turbulence depend on the nonstationarity of the forcing and the amplitude of pre-existing disturbances (Inoue & Smyth 2009). Turbulence may occur at large values of the Richardson number because the atmospheric boundary layer always contains finite-amplitude perturbations and is thus not a linear stability problem. The allowance of nonlinear effects leads to the growth of perturbations for even large Richardson numbers (Majda & Shefter 1998).

The turbulence and nonstationary of the nonturbulent flow continually interact (Derbyshire 1995a). Mahrt et al. (2013) found the maintenance of turbulence at large Richardson numbers

by submeso motions. Finnigan et al. (1984) explicitly showed turbulence at high Richardson numbers associated with unusually well-defined waves. Disturbances above the boundary layer, of unknown origin, might induce surface pressure perturbations and contribute to finite-amplitude wind fluctuations near the surface. As an additional source of turbulence, available potential energy of the perturbation flow can be converted back to turbulent kinetic energy at any Richardson number (Zilitinkevich et al. 2007).

Internal intermittency: intermittency resulting from interaction between the turbulence and the shear

Nappo (2012), Abarbanel et al. (1984), and Grisogono (1994) examined instability due to inflection points that may also contribute to turbulence at large Richardson numbers, even though such instability may be constrained by stratification (Grisogono 2011). Gage (1971) theoretically found that for a simple shear flow, inflection point instability increases the critical Richardson number, which in a more complex very stable boundary layer might augment turbulence for all Richardson numbers. Unfortunately, second-order derivatives computed from observed atmospheric profiles are vulnerable to large errors.

Even extremely weak slopes can generate intermittent drainage flow regardless of the Richardson number, which in turn can generate turbulence near the surface. For very stable conditions, minor surface heterogeneity of no consequence in the daytime boundary layer may induce instabilities and the generation of turbulence and effect the relationship between the area-averaged turbulence and the Richardson number for the area-averaged flow (Derbyshire 1995b).

4.4. Intermittency

The variability of the turbulence is sometimes posed in terms of intermittency indices, although the definition of intermittency varies between studies and disciplines and depends on scale as well. To some degree, all turbulence is intermittent. At the same time, the turbulence in the atmospheric stable boundary layer never vanishes. Mahrt (1989) distinguished between small-scale (or fine-scale) intermittency organized as a substructure of the main eddies and global intermittency associated with the organization of patches of eddies on scales that are large compared to the main eddy size. The atmospheric literature tends to focus on the latter.

Turbulence quantities, such as dissipation, may vary locally by orders of magnitude (Muschinski et al. 2004) associated with large regions of minimal turbulence and small regions of enhanced turbulent activity (Howell & Sun 1999, Yagüe et al. 2006). The mixing events in near-calm flow are less frequent than in most intermittency studies in the literature (Katul et al. 1994), yet they can still dominate the total vertical transport. Intermittency in the stable atmospheric boundary layer is not an on-off process. The frequency distribution of turbulence strength is not bimodal but is rather skewed toward larger values of the turbulence. As a result, the identification of turbulence events and definition of intermittency are sensitive to the choice of minimum threshold value for turbulence events (Nakamura & Mahrt 2005). Cava & Katul (2009) explored fine-scale intermittency in terms of clustering properties of sign switches of scalar fluctuations and examined potential scaling laws.

The observed mixing events can be generated at the surface or result from downward bursting of turbulence (Nappo 1991). The nature of these transient events is site dependent and precludes simple universal theories. Nonstationary submeso motions lead to externally forced intermittency of the turbulence. This contrasts with internal intermittency associated with the interplay among the turbulence, the mean shear, and stratification with fixed external forcing. In the case of internal intermittency, the shear builds (decreasing the Richardson number) and eventually augments the turbulence through shear instability. The resulting mixing reduces the shear, which increases the Richardson number and leads to turbulence decay. Percentage-wise, the shear varies much more than does the stratification and enters quadratically into the Richardson number. Van de Wiel

et al. (2012a) formulated a similar argument in terms of a maximum sustainable surface heat flux. Once this maximum is exceeded, the turbulence collapses, leading to flow acceleration, the regeneration of turbulence, and so forth. Liu et al. (2012) more specifically postulated internal cyclic behavior resulting from interaction between flow instability and turbulence. The growing shear due to unstable modes generates turbulence that damps the unstable modes, which in turn reduces shear, subsequently leading to turbulence decay, and so forth. In general, it has been difficult to isolate internal intermittency in the very stable boundary layer because the turbulence is generally nonstationary owing to external forcing by submeso motions. Nonetheless, internal intermittency has been identified in the very stable boundary layer (Fernando 2003, Pardyjak et al. 2002).

External intermittency: intermittency forced by nonstationary submeso shear

Internal intermittency may also appear in drainage flows. Downslope or downvalley flow can accelerate to the point of significant shear instability and mixing, which reduces the buoyancy deficit and momentum of the downslope flow. The subsequent reduction of downslope flow leads to a reduction of the turbulence, enhanced cooling of the surface flow, and acceleration of the downslope flow. This cycle leads to internal intermittency. The external intermittency of drainage flows forced by nonstationary motions in the submeso range (Helmis 1996, McNider et al. 1995, Monti et al. 2002) is probably more frequent than internal intermittency.

4.5. Transient Profile Distortion

For very stable conditions, the average of many vertical profiles is characterized by smooth height dependence and, in the absence of drainage flows, corresponds to shear decreasing systematically with height, as in Mahrt & Vickers (2006). However, individual wind profiles in the very stable boundary layer are often severely distorted on submeso timescales. Profile distortion includes transient near-surface wind maxima and shear reversal with height, significant directional shear, and anomalous profile curvature and inflection points. The short-term distortion of the vertical profiles may be responsible for much of the turbulence. Mahrt (2008) found enhanced turbulence for strongly stratified boundary layers when transient inflection points are present. Inflection point instability and the resulting turbulent mixing in turn may eliminate the inflection points. Presumably, the timescale of the inflection point must be as long as the turbulence adjustment timescale to significantly influence the turbulence.

5. SUBMESO MOTIONS

With very weak winds in the nocturnal boundary layer, turbulence generation seems to be associated primarily with submeso accelerations (Conangla et al. 2008, Mahrt et al. 2012). The turbulence is expected in turn to diffuse and exert drag on the submeso motions. Although submeso motions seem to always be present, their impact is limited primarily to weak-wind conditions (Anfossi et al. 2005). The strength of submeso motions based on cross-wind velocity variance is site dependent and tends to be greater in complex terrain (Vickers & Mahrt 2007).

Riley & Lelong (2000) and others partitioned the perturbation flow into turbulence, two-dimensional modes with potential vorticity, and propagating wave modes, in which the latter two categories fall under the general usage of the term submeso in the current review. I first survey the literature on common nonwave motions (Section 5.1) and then consider the more extensive literature on wave-like modes (Section 5.2).

5.1. Nonwave Modes

Two-dimensional modes with minimal vertical coherence are sometimes referred to as pancake motions or meandering modes, although the term meandering is sometimes reserved for space

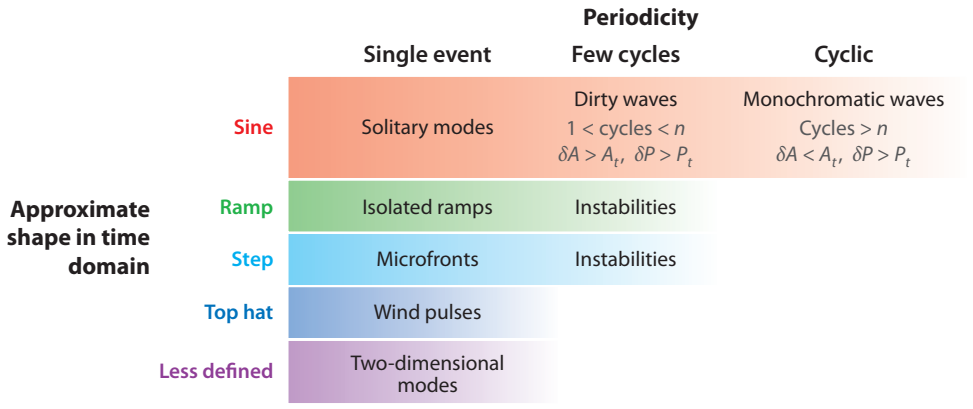

Figure 4

A schematic of different idealized shapes of structures found in time series. Unspecified n defines the minimum number of cycles required in order to be cyclic. A_t is the maximum allowed change of amplitude between subsequent cycles for potential inclusion into the cyclic category. P_t is the maximum change in period between subsequent cycles for potential inclusion into the cyclic category. The phase between variables is additional information not included here.

scales much larger than the largest boundary-layer eddies. Two-dimensional modes have been examined in a number of laboratory and numerical studies (Meunier et al. 2005, Riley & Lelong 2000, Waite & Bartello 2004). The interaction between laboratory gravity waves and two-dimensional modes was explored by Godoy-Diana et al. (2006).

Laboratory and numerically simulated two-dimensional modes can be characterized by significant vertical coherence, such as columnar vortices (Billant & Chomaz 2000) that are vulnerable to breakdown through instability. Such vertically coherent modes have not been observed in the atmospheric stable boundary layer.

Most evidence of two-dimensional modes from atmospheric data is more inferential (as in Anfossi et al. 2005, Kristensen et al. 1981, and Lilly 1983) and does not demonstrate that such vortices are actually resolved in the boundary layer. Our videos of natural and machine-generated fog, and attendant velocities derived from pattern recognition techniques, reveal occasional weak vortex motions on horizontal scales of tens to hundreds of meters in the very stable boundary layer (see **http://www.submeso.org**). Two-dimensional modes probably result from vertical decorrelation (Lilly 1983) owing to the conversion of vertical kinetic energy to potential energy in the presence of strong stable stratification.

Because atmospheric data do not allow an adequate evaluation of potential vorticity or the horizontal structure of the two-dimensional modes, motions in the stable atmospheric boundary layer are sometimes identified with coherent structures in time series, as summarized in **Figure 4**. Actual motions may have characteristics between the idealized modes and typically have structures that are more complex than the idealized signatures outlined in **Figure 4**. Although shapes are the normal and natural tool for phenomenologically identifying structures from time series, Belušić & Mahrt (2012) pointed out that similar shapes occur over a wide variety of scales and that physics cannot be attached to a certain shape without considering its scale. The terminology for different structures identified in time series varies among studies and may depend on the chosen variable.

Microfront: horizontal propagating narrow zones of strong horizontal gradients of wind or scalars over a couple of meters or less

In very stable conditions, even weak slopes can generate intermittent drainage flows, which appear as events in time series (Aubinet et al. 2003, Blumen 1984, Doran & Horst 1981). Buoyancy-driven drainage flows and density currents typically generate microfronts at their leading edge

(Blumen et al. 1999, Hohreiter 2008, Sun et al. 2002, Viana et al. 2010). The origin of density currents is generally not known. Microfronts may also occur in advance of warmer air. Mahrt (2010) suggested that downward advection/mixing of higher momentum and warmer temperatures could produce such warm microfronts.

Microfronts appear to be as common as sinusoidal signatures in the stable boundary layer (Belušić & Mahrt 2012). They can also be generated by surface wave amplification and steepening (Chimonas 1994), transient horizontal divergence and convergence driven by pressure disturbances of unknown origin, and surface heterogeneities that induce sharp horizontal differences during calm periods that are subsequently advected as microfronts.

Ramp structures are common in the stable boundary layer (Belušić & Mahrt 2012) and may occur in sequences of several events. Pulses of enhanced wind speed are represented in terms of a top-hat structure in **Figure 4** although they can be asymmetric. Here, they are differentiated from solitary modes because they do not appear to propagate. They seem to be more related to mixing events and downward transport of stronger horizontal momentum. Identifying signatures from time series reveals only limited inferences about the physics of the motions, so more detailed analyses using networks of data and new observational techniques are required (see Section 6).

5.2. Classification of Observed Wave-Like Motions

Examples of well-defined large waves can be found in the middle and upper troposphere (Zhang et al. 2001). Even the casual ground observer can sometimes see well-defined wave modes in altostratus and cirrus clouds that may include more than ten wavelengths. Wave-like motions are also common in the stable atmospheric boundary layer on a wide variety of scales. However, gravity waves are less clearly defined near the surface, partly because of weak vertical motions. In addition, interaction with the rough ground surface and typical heterogeneity may lead to more complex generation of superimposed waves and complex wave reflection. Nonetheless, observations of the stable boundary layer from various data sets generally show abundant wave-like behavior even near the surface. Strong stratification in the stable boundary layer can lead to effective ducting of waves (Fritts et al. 2003, Nappo 2012). Ducted waves may propagate long distances and may be observed far from their unknown source (Viana et al. 2009).

Numerically separating turbulence and waves from time series is substantially more difficult than recognizing the mere existence of wave-like motions (Stewart 1969). The literature presumably emphasizes those cases in which spectral gaps or phase relationships between variables are well defined and separation between waves and turbulence becomes locally possible (Caughey & Readings 1975, Hunt et al. 1985, Lu et al. 1983). Caughey & Readings (1975) indicated that spectral analysis cannot be useful unless waves and turbulence have very different frequency bands, which is often not the case in the stable boundary layer. Band-passed filters are used to eliminate turbulence and longer waves. However, the bandwidth must be sufficiently broad to avoid creating waves from noise. Because wave-like motions generally occur in local packets in the stable boundary layer and the turbulence is not periodic, various wavelet techniques and multiresolution decomposition appear to be superior to global Fourier decompositions for separating wave and turbulent motions (Cuxart et al. 2002, Terradellas et al. 2001, Viana et al. 2010).

Most atmospheric observations do not include adequate information to estimate the wavelength or phase propagation vector. As a result, signatures that are sine-like in time series and include at least a couple of cycles are referred to as "waves" in the boundary-layer literature. This casual terminology is used here, subject to the following classification.

First, monochromatic waves of more than a few periods with approximately constant period and amplitude are infrequently observed in atmospheric stable boundary layers. Second, most

Dirty waves: packets of wave-like motions whose amplitude and period vary substantially between adjacent cycles

Soliton: a propagating sign-like structure with a single cycle; variants are widespread

wave-like phenomena near the surface change their amplitude and period substantially from one wave period to the next, and only a few cycles can be observed. The amplitude often varies more than the period, as is evident by inspecting figures in literature (Anderson 2003, Caughey & Readings 1975, Lee et al. 1997), although there are many examples in which both the amplitude and period vary significantly between sequential periods (Cuxart et al. 2002, DeBaas & Driedonks 1985, Einaudi & Finnigan 1993, Meillier et al. 2008, Viana et al. 2010). Other wave-like signatures are significantly asymmetric and may approach ramp-like structures. I collectively and leniently refer to these common signatures of variable amplitude and period as dirty waves (**Figure 4**). The local nature of the wave packet, the variability between sequential periods, and deviations from the sine shape all lead to wide spreading of variance in frequency and wave-number space (Tennekes 1976). Dirty waves fail to satisfy the linear theories based on the Taylor-Goldstein equation (Nappo 2012) because the background flow varies on timescales that are not large compared to the wave itself.

Third, the terminology and suspected dynamics of solitary waves and solitons vary in the literature (Christie et al. 1978, Rao et al. 2004, Rees et al. 1998). Solitary modes (Anderson 2003, Sun et al. 2002, 2004, Terradellas et al. 2005) are frequently observed in the stable atmospheric boundary layer, although their cause is generally unknown. Rees et al. (1998, 2000) found that solitary waves are common within the surface inversion with weak winds, even over simple surfaces, and can propagate at speeds of 10–20 m s^{-1} or more. Such modes can be much deeper than the depth of typical tall towers and can trigger local density currents (Mahrt 2010). Such fast-moving waves would appear with a small timescale at a fixed point, even though they have large wavelengths.

Finally, the majority of the wave-like motions in the nocturnal boundary layer involve the superposition of wave modes such that individual wave modes are difficult to isolate from the data. Observations of this common stochastic wave state have not been examined in the literature. However, even the classical pictures of coherent clean waves based on acoustic sounders include periods of more stochastic wave-like motion, as in Hooke & Jones (1986, figure 1) and Li et al. (1983, figure 2). It is not known if the complex signatures mainly result from the superposition of different modes or if the individual modes are themselves complex. Such complexity contributes to difficulties in separating waves and turbulence from observed atmospheric observations.

5.3. Potential Causes of Waves

Although the source of wave-like motions near the surface is generally unknown, various mechanisms have been proposed. For example, waves are often generated by topography whose depth scale may be substantially deeper than the thin nocturnal boundary layer (Smith 2007). Such waves generally extend downward through the boundary layer and may be influenced by surface stress.

Waves may also be generated by flow over smaller-scale topography and obstacles whose depth is smaller than the boundary-layer depth. From simple linear theory, surface obstacles and topographical features are expected to generate propagating gravity waves when the advective time, required for the flow to pass the surface feature, is longer than the buoyancy timescale. The interpretation of such theories for actual stable boundary layers is uncertain because of heterogeneity and complex vertical structure, including rapidly decreasing N with height.

Advancing microfronts and mesoscale fronts can induce gravity waves. Tjernström & Mauritsen (2009) found gravity waves in advance of mesoscale fronts. Using observations and numerical simulations, Nappo et al. (2008), Viana et al. (2010), and Udina et al. (2013) found gravity waves following a density current, evident at the interfacial top of the cold air. Porch et al. (1991) suspected that oscillations in a valley were initiated by the interaction between downvalley flow in the cold pool and tributary flow into the valley. The interaction of gravity waves and density currents was

examined by Viana et al. (2009) and Terradellas et al. (2005). Chemel et al. (1991) showed that nonstationary drainage flows in a valley can initiate nonpropagating buoyancy oscillations that become trapped by a critical level.

Fluctuating surface pressure associated with disturbances aloft induces surface motions (Viana et al. 2009). Waves at the top or above the boundary layer may modulate the wind field even in neutral and convective boundary layers. Waves in the latter class are sometimes classified as convection waves (Keuttner et al. 1993) and have been more recently examined by Böhme et al. (2004) and Gibert et al. (2011).

Inflection point instability may induce common wave-like motions above tall canopies (Finnigan 2000) in which wave-like motions can extend over many periods (Lee & Barr 1998, van Gorsel et al. 2011). Kelvin-Helmholtz instability also initiates periodic instabilities in stratified flow that could be included in the terminology wave-like motions.

According to Jeffries' mechanism, the surface stress amplifies wave growth (Pulido & Chimonas 2001). At the same time, turbulence may reduce wave activity through diffusion of the wave energy (Lee et al. 1997).

5.4. The Influence of Waves on the Stable Boundary Layer

Although atmospheric work has mainly concentrated on the generation of turbulence by waves, an alternative viewpoint focuses on the generation of waves by the turbulence (Gibson 1999, Stewart 1969). The size of the turbulent eddies in the very stable atmospheric boundary layer is probably not of sufficient horizontal scale to trigger gravity waves. Wave motions can trigger turbulence by periodically increasing the flow speed and shear at the surface and reducing the local Richardson number (Nappo 2012). After surveying a large number of oceanographic papers, Smyth & Moum (2012) found that Kelvin-Helmholtz instability is a key link in the generation of turbulence by wave motions.

At the ground surface with weak atmospheric winds, waves can periodically generate a low-level wind maximum, which might enhance the shear generation of fine-scale turbulence as well as induce an inflection point in the overlying flow. Although there are numerous examples of semiperiodic near-surface wind maxima, such observations have not yet been reported in the literature. Because wave motions are nonlocal, the generation of turbulence by wave motions cannot be expected to obey similarity theory (Finnigan 1999). Even if the wave motions can be included as a deterministic part of the mean flow, the turbulence generated by such waves will be in approximate equilibrium only if the wave period is large compared to the turbulence adjustment timescale. Conversely, waves can also increase the stability of the flow and thus reduce existing turbulence (Viana et al. 2009).

Wave-like motions may also transport momentum (Fernando & Weil 2010, Sukorianski et al. 2009) and possibly scalars. However, estimates of fluxes on the wave scale from atmospheric data are usually problematic because of severe sampling errors. The concept of random flux errors has no formal mathematical support for nonstationary time series. In addition, wave-like motions near the surface are often characterized by low attack angles with respect to a horizontal surface, in which case even small misalignment of the sonic anemometers can lead to large relative errors.

6. SUMMARY: THE STOCHASTIC MIX

The analysis of observations of the stable atmospheric boundary layer in the literature has concentrated on weakly stable boundary layers that are reasonably well defined in terms of the

vertical structure of the mean flow and turbulence. In contrast, common very stable boundary layers include complex interactions between turbulence and wave-like and other submeso motions that are poorly understood. Classifying the boundary layer into just two simple regimes is a severe simplification but serves to highlight the main influences of the stability on the turbulence and vertical structure of the stable boundary layer. The very stable regime occurs with weak large-scale flow and strong stratification normally resulting from strong net radiative cooling of the surface, but also produced by the flow of warm air over much cooler surfaces. The turbulence generally fails to achieve equilibrium with constantly changing submeso motions. The vertical structure of the turbulence may assume a variety of forms, often with an increase of turbulence with height, reaching a maximum above the surface inversion. In the very stable boundary layer, local circulations can be induced by even weak topography and surface heterogeneity, often occurring simultaneously on multiple scales.

The submeso motions, as well as nonstationary radiative forcing of the surface due to variable cloud cover, are not deterministic. As a result, the stochastic turbulence becomes forced by a stochastic process in contrast to boundary layers forced by stationary homogeneous mean flow that obeys similarity theory. As examples of stochastic formulation of the forcing, Farrell & Ioannou (2008) introduced a stochastic wind field to study the response of sea-surface waves, and Bakas & Ioannou (2007) examined gravity waves forced by randomly generated temperature and vorticity fluctuations. Stochastic approaches, or a more complete similarity theory, might serve as a useful framework for the very stable regime. Patching of existing similarity theory is either unsuccessful or site dependent.

Improved understanding of local circulations and submeso motions can take advantage of new measurement techniques that provide detailed spatial variation on scales from 1 m to several kilometers. Such techniques include more extensive local networks of turbulence measurements and accurate fast-response pressure sensors; fiber-optic technology that includes fast-response cross sections (Thomas et al. 2012); and rapidly improving, remotely controlled aircraft (Bonin et al. 2013, Reuder et al. 2012). Such observations will supplement the current observations that are almost completely in the time domain (time series). Observations in the space domain provide better separation between turbulence and waves and are more useful for an examination of the main theories and concepts posed in the space domain, including the need for the estimation of turbulent length scales, wavelengths, and nonperiodic horizontal scales. These advances offer exciting opportunities for improving our understanding of the complex very stable regime.

SUMMARY POINTS

1. Turbulence in very stable conditions is poorly understood and does not categorically satisfy traditional definitions of turbulence.
2. Patching existing similarity theory does not seem useful for the very stable boundary layer.
3. In very stable conditions, the turbulence and the nonturbulent flow are generally nonstationary, and the turbulence is not in equilibrium with the nonturbulent flow.
4. The very stable boundary layer may assume a variety of different vertical structures, including near-surface wind maxima, inflection points, and maximum turbulence near the top of the surface inversion layer.

5. In very stable conditions, the turbulence may be generated primarily by shear associated with submeso motions that include wave-like modes, solitary waves, two-dimensional modes (pancake eddies, meandering motions), microfronts, and numerous more complex signatures.
6. Wave-like motions, microfronts, and intermittent drainage flows all interact within the very stable regime.

FUTURE ISSUES

1. Can the complex origin of wave-like motions near the surface be at least partially understood?
2. When are wave-like motions and other submeso motions the dominant source for turbulence generation in the strongly stratified boundary layer?
3. Can submeso motions be stochastically parameterized and related to local surface conditions, topography, and background atmospheric conditions?
4. Current strategies for field observations of the very stable boundary layer need to be substantially expanded with much better measurement of the horizontal structure.
5. The loss of information on the fine-scale turbulence due to sonic path-length averaging needs to be ameliorated by shorter sonic path lengths, improved hot-film anemometry, or new observational approaches.
6. Can the constant change of wind direction, resulting from submeso motions in weak-wind conditions, be parameterized for the prediction of horizontal dispersion?
7. Can the vertical scale of shear instabilities be estimated from observations?
8. Is the intermittency of turbulence and local circulations, such as drainage flows, primarily a result of external intermittency forced by submeso motions?

DISCLOSURE STATEMENT

The author is not aware of biases that might be perceived as affecting the objectivity of this review.

ACKNOWLEDGMENTS

The helpful comments of Danijel Belušić and James Riley are greatly appreciated. This project received support from the National Science Foundation through grant AGS-1115011.

LITERATURE CITED

Abarbanel H, Holm D, Marsden J, Ratiu T. 1984. Richardson number criterion for the nonlinear stability of three-dimensional stratified flow. *Phys. Rev. Lett.* 52:2352–55

Anderson P. 2003. Fine-scale structure observed in a stable atmospheric boundary layer by Sodar and kite-borne tethersonde. *Bound.-Layer Meteorol.* 107:323–51

Anderson P. 2009. Measurement of Prandtl number as a function of Richardson number avoiding self-correlation. *Bound.-Layer Meteorol.* 131:345–62

Andreas EL, Claffey K, Makshtas A. 2000. Low-level atmospheric jets and inversions over the western Weddell Sea. *Bound.-Layer Meteorol.* 97:459–86

Anfossi D, Oetti D, Degrazia G, Boulart A. 2005. An analysis of sonic anemometer observations in low wind speed conditions. *Bound.-Layer Meteorol.* 114:179–203

Anquetin A, Guilbaud C, Chollet JP. 1998. The formation and destruction of inversion layers within a deep valley. *J. Appl. Meteorol.* 37:1547–60

Aubinet M, Heinesch B, Yernaux M. 2003. Horizontal and vertical CO_2 advection in a sloping forest. *Bound.-Layer Meteorol.* 108:397–417

Baas P, Steeneveld G, van de Weil B, Holtslag A. 2006. Exploring self-correlation in the flux-gradient relationships for stably stratified conditions. *J. Atmos. Sci.* 63:3045–54

Bakas NA, Ioannou PJ. 2007. Momentum and energy transport by gravity waves in stochastically driven stratified flows. Part I: radiation of gravity waves from a shear layer. *J. Atmos. Sci.* 64:1509–29

Balsley B, Frehlich R, Jensen ML, Meillier Y. 2003. Extreme gradients in the nocturnal boundary layer: structure, evolution and potential causes. *J. Atmos. Sci.* 60:2496–508

Balsley B, Frehlich RG, Jensen ML, Meillier Y. 2006. High-resolution in situ profiling through the stable boundary layer: examination of the SBL top in terms of minimum shear, maximum stratification, and turbulence decrease. *J. Atmos. Sci.* 63:1291–307

Banta R, Pichugina Y, Brewer W. 2006. Turbulent velocity-variance profiles in the stable boundary layer generated by a nocturnal low-level jet. *J. Atmos. Sci.* 63:2700–19

Basu S, Porté-Agel F, Foufoula-Georgiou E, Vinuesa JF, Pahlow M. 2006. Revisiting the local scaling hypothesis in stably stratified atmospheric boundary-layer turbulence: an integration of field and laboratory measurements with large-eddy simulations. *Bound.-Layer Meteorol.* 119:473–500

Belušić D, Mahrt L. 2012. Is geometry more universal than physics in atmospheric boundary layer flow? *J. Geophys. Res.* 117:D09115

Billant P, Chomaz JM. 2000. Experimental evidence for a new instability of a vertical columnar vortex pair in a strongly stratified fluid. *J. Fluid Mech.* 418:167–88

Blumen W. 1984. An observational study of instability and turbulence in nighttime drainage winds. *Bound.-Layer Meteorol.* 28:245–69

Blumen W, Grossman R, Piper M. 1999. Analysis of heat budget, dissipation and frontogenesis in a shallow density current. *Bound.-Layer Meteorol.* 91:281–306

Böhme T, Hauf T, Lehmann V. 2004. Investigation of short-period gravity waves with the Lindenberg 482 MHz tropospheric wind profiler. *Q. J. R. Meteorol. Soc.* 130:2933–52

Bonin T, Chilson P, Zielke B, Fedorovich E. 2013. Observations of the early evening boundary-layer transition using a small unmanned aerial system. *Bound.-Layer Meteorol.* 146:119–32

Brown R. 1972. On the inflection point instability of a stratified Ekman boundary layer. *J. Atmos. Sci.* 29:850–59

Burns S, Sun J, Delany A, Semmer S, Oncley S, Horst T. 2003. A field intercomparison technique to improve the relative accuracy of longwave radiation measurements and an evaluation of CASES-99 pyrgeometer data quality. *J. Atmos. Ocean. Technol.* 20:348–61

Busch NE, Vinnichenko NK, Waterman AT Jr, Beard C, Stewart RW, Scotti RS. 1969. Waves and turbulence. *Radio Sci.* 4:1377–79

Caughey S, Readings C. 1975. An observation of waves and turbulence in the earth's boundary layer. *Bound.-Layer Meteorol.* 9:279–96

Cava D, Giostra U, Siqueira M, Katul G. 2004. Organized motion and radiative perturbations in the nocturnal canopy sublayer above an even-aged pine forest. *Bound.-Layer Meteorol.* 112:129–57

Cava D, Katul G. 2009. The effects of thermal stratification on clustering properties of canopy turbulence. *Bound.-Layer Meteorol.* 130:307–25

Chemel C, Staquet C, Largeron Y. 1991. Generation of internal gravity waves by a katabatic wind in an idealized alpine valley. *Meteorol. Atmos. Phys.* 103:187–94

Chimonas G. 1994. Jeffrey's drag instability applied to waves in the lower atmosphere: linear and nonlinear growth rates. *J. Atmos. Sci.* 51:3758–74

Christie DR, Muirhead KJ, Hales AL. 1978. Long nonlinear waves in the lower atmosphere. *J. Atmos. Sci.* 35:805–25

Conangla L, Cuxart J, Soler MR. 2008. Characterisation of the nocturnal boundary layer at a site in northern Spain. *Bound.-Layer Meteorol.* 128:255–76

Cuxart J, Morales G, Terradellas E, Yagüe C. 2002. Study of coherent structures and estimation of the pressure transport terms for the nocturnal boundary layer. *Bound.-Layer Meteorol.* 105:305–28

DeBaas AF, Driedonks AGM. 1985. Internal gravity waves in a stably-stratified boundary layer. *Bound.-Layer Meteorol.* 31:303–23

Derbyshire H. 1995a. Stable boundary layers: observations, models and variability part I: modelling and measurements. *Bound.-Layer Meteorol.* 74:19–54

Derbyshire H. 1995b. Stable boundary layers: observations, models and variability part II: data analysis and averaging effects. *Bound.-Layer Meteorol.* 75:1–24

Doran JC, Horst TW. 1981. Velocity and temperature oscillations in drainage winds. *J. Appl. Meteorol.* 20:360–64

Duynkerke P. 1999. Turbulence, radiation and fog in Dutch stable boundary layers. *Bound.-Layer Meteorol.* 90:447–77

Einaudi F, Finnigan JJ. 1993. Wave-turbulence dynamics in the stably stratified boundary layer. *J. Atmos. Sci.* 50:1842–64

Farrell BF, Ioannou PJ. 2008. The stochastic parametric mechanism for growth of wind-driven surface water waves. *J. Phys. Oceanogr.* 38:862–79

Fernando HJS. 2003. Turbulence patches in a stratified shear flow. *Phys. Fluids* 15:3164–69

Fernando HJS, Weil JC. 2010. Whither the stable boundary layer? A shift in the research agenda. *Bull. Am. Meteorol. Soc.* 91:1475–84

Finnigan J. 1999. A note on wave-turbulence interaction and the possibility of scaling the very stable boundary layer. *Bound.-Layer Meteorol.* 90:529–39

Finnigan J. 2000. Turbulence in plant canopies. *Agric. For. Meteorol.* 32:519–71

Finnigan J, Einaudi F, Fua D. 1984. The interaction between an internal gravity wave and turbulence in the stably-stratified nocturnal boundary layer. *J. Atmos. Sci.* 41:2409–36

Flores O, Riley J. 2011. Analysis of turbulence collapse in the stably stratified surface layer using direct numerical simulation. *Bound.-Layer Meteorol.* 139:241–59

Foster RC, Levy G. 1998. The contribution of organized roll vortices to the surface wind vector in baroclinic conditions. *J. Atmos. Sci.* 55:1466–72

Fritts D, Nappo C, Riggin D, Balsley B, Eichinger W, Newsom R. 2003. Analysis of ducted motions in the stable boundary layer during CASES-99. *J. Atmos. Sci.* 60:2450–72

Gage K. 1971. The effect of stable thermal stratification on the stability of viscous parallel flows. *J. Fluid Mech.* 47:1–20

Galperin B, Sukoriansky S, Anderson P. 2007. On the critical Richardson number in stably stratified turbulence. *Atmos. Sci. Lett.* 8:65–69

Garratt J. 1992. *The Atmospheric Boundary Layer.* Cambridge, UK: Cambridge Univ. Press

Gerz T, Howell JF, Mahrt L. 1994. Vortex stretching and microfronts. *Phys. Fluids A* 6:1242–51

Gibert F, Arnault N, Cuesta J, Plougonven R, Flammant P. 2011. Internal gravity waves convectively forced in the atmospheric residual layer during the morning transition. *Q. J. R. Meteorol. Soc.* 137:1610–24

Gibson C. 1999. Fossil turbulence revisited. *J. Mar. Sys.* 21:147–67

Godoy-Diana R, Chomaz JM, Donnadieu C. 2006. Internal gravity waves in a dipolar wind: a wave-vortex interaction experiment in a stratified fluid. *J. Fluid Mech.* 548:281–308

Grachev A, Andreas E, Fairall C, Guest P, Persson P. 2013. The critical Richardson number and limits of applicability of local similarity theory in the stable boundary layer. *Bound.-Layer Meteorol.* 147:51–82

Grachev A, Fairall C, Persson P, Andreas E, Guest P. 2005. Stable boundary-layer scaling regimes: the SHEBA data. *Bound.-Layer Meteorol.* 116:201–35

Grisogono B. 1994. A curvature effect on the critical Richardson number. *Croat. Meteorol. J.* 29:43–46

Grisogono B. 2011. The angle of near-surface wind-turning in weakly stable boundary layers. *Q. J. R. Meteorol. Soc.* 137:700–8

Helmis C. 1996. Some aspects of the variation with time of katabatic flow over a simple slope. *Q. J. R. Meteorol. Soc.* 122:595–610

Hicks B. 1978. Some limitations of dimensional analysis and power laws. *Bound.-Layer Meteorol.* 14:567–69
Hohreiter V. 2008. Finescale structure and dynamics of an atmospheric temperature interface. *Q. J. R. Meteorol. Soc.* 65:1701–10
Hooke WH, Jones RM. 1986. Dissipative waves excited by gravity wave encounters with the stably stratified planetary boundary layer. *J. Atmos. Sci.* 43:2048–60
Hopfinger EJ. 1987. Turbulence in stratified fluids: a review. *J. Geophys. Res.* 92:5287–303
Howell J, Sun J. 1999. Surface layer fluxes in stable conditions. *Bound.-Layer Meteorol.* 90:495–520
Hunt J, Kaimal J, Gaynor J. 1985. Some observations of turbulence structure in stable layers. *Q. J. R. Meteorol. Soc.* 111:793–815
Hunt J, Vassilicos J. 1991. Kolmogorov's contributions to the physical and geometrical understanding of small-scale turbulence and recent developments. *Proc. R. Soc. Lond. A* 434:183–210
Inoue R, Smyth WD. 2009. Efficiency of mixing forced by unsteady shear flow. *J. Phys. Oceanogr.* 39:1150–66
Katul G, Albertson J, Parlange M, Chu CR, Stricker H. 1994. Conditional sampling, bursting and the intermittent structure of sensible heat flux. *J. Geophys. Res.* 99:22869–76
Katul G, Hsieh CI, Bowling D, Clark K, Shurpali N, et al. 1999. Spatial variability of turbulent fluxes in the roughness sublayer of an even-aged pine forest. *Bound.-Layer Meteorol.* 93:1–28
Keuttner J, Hildebrand P, Clark T. 1993. Convection waves: observations of gravity wave systems over convectively active boundary layers. *Q. J. R. Meteorol. Soc.* 113:445–67
Klipp C, Mahrt L. 2004. Flux-gradient relationship, self-correlation and intermittency in the stable boundary layer. *Q. J. R. Meteorol. Soc.* 130:2087–104
Kristensen L, Jensen N, Peterson EL. 1981. Lateral dispersion of pollutants in a very stable atmosphere: the effect of the meandering. *Atmos. Environ.* 15:837–44
Lee X, Barr A. 1998. Climatology of gravity waves in a forest. *Q. J. R. Meteorol. Soc.* 124:1403–19
Lee X, Neuman H, den Hartog G, Fuentes J, Black T, et al. 1997. Observations of gravity waves in a boreal forest. *Bound.-Layer Meteorol.* 84:383–98
Li XS, Gaynor JE, Kaimal JC. 1983. A study of multiple stable layers in the nocturnal lower atmosphere. *Bound.-Layer Meteorol.* 26:157–68
Lilly D. 1983. Stratified turbulence and the mesoscale variability of the atmosphere. *J. Atmos. Sci.* 40:749–61
Liu Z, Thorpe SA, Smyth WD. 2012. Instability and hydraulics of turbulent stratified shear flows. *J. Fluid Mech.* 695:235–56
Lu NP, Neff WD, Kaimal JC. 1983. Wave and turbulence structure in a disturbed nocturnal inversion. *Bound.-Layer Meteorol.* 26:141–55
Luhar A, Hurley P, Rayner K. 2009. Modeling near-surface low winds over land under stable conditions: sensitivity tests, flux-gradient relationships and stability parameters. *Bound.-Layer Meteorol.* 130:249–74
Mahrt L. 1989. Intermittency of atmospheric turbulence. *J. Atmos. Sci.* 46:79–95
Mahrt L. 2008. The influence of transient flow distortion on turbulence in stable weak-wind conditions. *Bound.-Layer Meteorol.* 127:1–16
Mahrt L. 2010. Common microfronts and other solitary events in the nocturnal boundary layer. *Q. J. R. Meteorol. Soc.* 136:1712–22
Mahrt L, Howell J. 1994. The influence of coherent structures and microfronts on scaling laws using global and local transforms. *J. Fluid Mech.* 260:247–70
Mahrt L, Richardson S, Seaman N, Stauffer D. 2012. Turbulence in the nocturnal boundary layer with light and variable winds. *Q. J. R. Meteorol. Soc.* 138:1430–39
Mahrt L, Thomas C, Richardson S, Seaman N, Stauffer D, Zeeman M. 2013. Non-stationary generation of weak turbulence for very stable and weak-wind conditions. *Bound.-Layer Meteorol.* 147:179–99
Mahrt L, Vickers D. 2002. Contrasting vertical structures of nocturnal boundary layers. *Bound.-Layer Meteorol.* 105:351–63
Mahrt L, Vickers D. 2006. Extremely weak mixing in stable conditions. *Bound.-Layer Meteorol.* 119:19–39
Majda A, Shefter M. 1998. Elementary stratified flows with instability at large Richardson number. *J. Fluid Mech.* 376:319–50
McNaughton KG. 2012. The flow of mechanical energy in convective boundary layers. *Bound.-Layer Meteorol.* 145:145–63

McNider R, England D, Friedman M, Shi X. 1995. Predictability of the stable atmospheric boundary layer. *J. Atmos. Sci.* 52:1602–14
Meillier Y, Frehlich RG, Jones RM, Balsley BB. 2008. Modulation of small-scale turbulence by ducted gravity waves in the nocturnal boundary layer. *J. Atmos. Sci.* 65:1414–27
Meunier P, Dizés SL, Leweke T. 2005. Physics of vortex merging. *C. R. Phys.* 6:431–50
Monti PF, Chan W, Princevac M, Kowalewski T, Pardyjak E. 2002. Observations of flow and turbulence in the nocturnal boundary layer over a slope. *J. Atmos. Sci.* 59:2513–34
Mukund V, Singh DK, Ponnulakshmi VK, Subramanian G, Sreenivas KR. 2013. Field and laboratory experiments on aerosol-induced cooling in the nocturnal boundary layer. *Q. J. R. Meteorol. Soc.* In press
Muschinski A, Frehlich R, Balsley B. 2004. Small-scale and large-scale intermittency in the nocturnal boundary layer and the residual layer. *J. Fluid Mech.* 515:319–51
Nakamura R, Mahrt L. 2005. A study of intermittent turbulence with CASES-99 tower measurements. *Bound.-Layer Meteorol.* 114:367–87
Nappo CJ. 1991. Sporadic breakdown of stability in the PBL over simple and complex terrain. *Bound.-Layer Meteorol.* 54:69–87
Nappo CJ. 2012. *An Introduction to Atmospheric Gravity Waves*. New York: Academic. 359 pp. 2nd ed.
Nappo CJ, Miller DR, Hiscox AL. 2008. Wave-modified flux and plume dispersion in the stable boundary layer. *Bound.-Layer Meteorol.* 129:211–23
Ohya Y, Nakamura R, Uchida T. 2008. Intermittent bursting of turbulence in a stable boundary layer with low-level jet. *Bound.-Layer Meteorol.* 126:249–63
Panofsky H, Dutton J. 1984. *Atmospheric Turbulence: Models and Methods for Engineering Applications.* New York: Wiley
Pardyjak E, Monti P, Fernando HJS. 2002. Flux Richardson number measurements in stable atmospheric shear flows. *J. Fluid Mech.* 449:307–16
Porch W, Clements W, Coulter R. 1991. Nighttime valley waves. *J. Appl. Meteorol.* 30:145–56
Pulido M, Chimonas G. 2001. Forest canopy waves: the long-wavelength component. *Bound.-Layer Meteorol.* 100:209–24
Rao M, Castracane P, Fua D, Fiocco G. 2004. Observations of atmospheric solitary waves in the urban boundary layer. *Bound.-Layer Meteorol.* 111:85–108
Rees J, Anderson P, King J. 1998. Observations of solitary waves in the stable atmospheric boundary layer. *Bound.-Layer Meteorol.* 86:47–61
Rees J, Denholm-Price J, King J, Anderson P. 2000. A climatological study of internal gravity waves in the atmospheric boundary layer overlying the Brunt Ice Shelf, Antarctica. *J. Atmos. Sci.* 57:511–26
Reuder J, Jonassen M, Olafsson H. 2012. The Small Unmanned Meteorological Observer SUMO: recent developments and applications of a micro-UAS for atmospheric boundary layer research. *Acta Geophys.* 60:1454–73
Riley JJ, Lelong MP. 2000. Fluid motions in the presence of strong stable stratification. *Annu. Rev. Fluid Mech.* 32:613–57
Riley JJ, Lindborg E. 2008. Stratified turbulence: a possible interpretation of some geophysical turbulence measurements. *J. Atmos. Sci.* 65:2416–24
Smedman AS. 1988. Observations of a multi-level turbulence structure in a very stable atmospheric boundary layer. *Bound.-Layer Meteorol.* 44:231–53
Smedman AS, Tjernström H, Högström U. 1993. Analysis of the turbulence structure of a marine low-level jet. *Bound.-Layer Meteorol.* 66:105–26
Smith RB. 2007. Interacting mountain waves and boundary layers. *J. Atmos. Sci.* 64:594–607
Smyth W, Moum JN. 2012. Ocean mixing by Kelvin-Helmholtz instability. *Oceanography.* 25:140–49
Sorbjan Z. 1989. *Structure of the Atmospheric Boundary Layer.* Englewood Cliffs, NJ: Prentice Hall
Sorbjan Z. 2010. Gradient-based scales and similarity laws in the stable boundary layer. *Q. J. R. Meteorol. Soc.* 136:1243–54
Stewart RW. 1969. Turbulence and waves in a stratified atmosphere. *Radio Sci.* 4:1269–78
Stull R. 1988. *An Introduction to Boundary Layer Meteorology*. Dordrecht: Kluwer Acad.
Sukorianski S, Dikovskaya N, Galperin B. 2009. Transport of momentum and scalar in turbulent flows with anisotropic dispersive waves. *Geophys. Res. Lett.* 36:L14609

Sukorianski S, Galperin B. 2013. An analytical theory of the buoyancy: Kolmogorov subrange transition in turbulent flows with stable stratification. *Philos. Trans. R. Lond. Ser. A* 371:20120212

Sun J, Burns S, Lenschow D, Banta R, Newsom R, et al. 2002. Intermittent turbulence associated with a density current passage in the stable boundary layer. *Bound.-Layer Meteorol.* 105:199–219

Sun J, Lenschow DH, Burns SP, Banta RM, Newsom RK, et al. 2004. Atmospheric disturbances that generate intermittent turbulence in nocturnal boundary layers. *Bound.-Layer Meteorol.* 110:255–79

Sun J, Mahrt L, Banta R, Pichugina Y. 2012. Turbulence regimes and turbulence intermittency in the stable boundary layer during CASES-99. *J. Atmos. Sci.* 69:338–51

Tennekes H. 1976. Fourier-transform ambiguity in turbulence dynamics. *J. Atmos. Sci.* 32:1660–63

Tennekes H, Lumley J. 1972. *A First Course in Turbulence.* Cambridge, MA: MIT Press

Terradellas E, Morales G, Cuxart J, Yagüe C. 2001. Wavelet methods: application to the study of the stable atmospheric boundary layer. *Dyn. Atmos. Oceans* 34:225–44

Terradellas E, Soler M, Ferreres E, Bravo M. 2005. Analysis of oscillations in the stable boundary layer using wavelet methods. *Bound.-Layer Meteorol.* 114:489–518

Thomas C, Kennedy A, Selker J, Moretti A, Schroth M, et al. 2012. High-resolution fibre-optic temperature sensing: a new tool to study the two-dimensional structure of atmospheric surface-layer flow. *Bound.-Layer Meteorol.* 142:177–92

Tjernström M, Balsley BB, Svensson G, Nappo C. 2009. The effects of critical layers on residual layer turbulence. *J. Atmos. Sci.* 66:468–80

Tjernström M, Mauritsen T. 2009. Mesoscale variability in the summer Arctic boundary layer. *Bound.-Layer Meteorol.* 130:383–406

Udina M, Soler M, Viana S, Yagüe C. 2013. Model simulation of gravity waves triggered by a density current. *Q. J. R. Meteorol. Soc.* 139:701–14

van de Wiel BJH, Moene A, Hartogenesis G, Bruin HD, Holtslag AAM. 2003. Intermittent turbulence in the stable boundary layer over land. Part III: a classification for observations during CASES-99. *J. Atmos. Sci.* 60:2509–22

van de Wiel BJH, Moene AF, Jonker HJJ. 2012a. The cessation of continuous turbulence as precursor of the very stable nocturnal boundary layer. *J. Atmos. Sci.* 69:3097–115

van de Wiel BJH, Moene AF, Jonker HJJ, Baas P, Basu S, et al. 2012b. The minimum wind speed for sustainable wind speed in the nocturnal boundary layer. *J. Atmos. Sci.* 69:3116–27

van de Wiel BJH, Moene AF, Steeneveld GJ, Baas P, Bosveld FC, Holtslag AAM. 2010. A conceptual view on inertial oscillations and nocturnal low-level jets. *J. Atmos. Sci.* 67:2679–89

van Gorsel E, Harman IN, Finnigan JJ, Leuning R. 2011. Decoupling of air flow above and in plant canopies and gravity waves affect micrometeorological estimates of net scalar exchange. *Agric. For. Meteorol.* 151:927–33

Vassilicos JC, Hunt J. 1978. Fractal dimensions and spectra of interfaces with application to turbulence. *Proc. R. Soc. Lond. A* 435:505–34

Viana S, Terradellas S, Yagüe C. 2010. Analysis of gravity waves generated at the top of a drainage flow. *J. Atmos. Sci.* 67:3949–66

Viana S, Yagüe C, Maqueda G. 2009. Propagation and effects of a mesoscale gravity wave over a weakly-stratified stable boundary layer during SABLES2006 field campaign. *Bound.-Layer Meteorol.* 133:165–88

Vickers D, Mahrt L. 2007. Observations of the cross-wind velocity variance in the stable boundary layer. *Environ. Fluid Mech.* 7:55–71

Waite M, Bartello P. 2004. Stratified turbulence dominated by vortical motion. *J. Fluid Mech.* 517:281–308

Weinstock J. 1985. On the theory of temperature spectra in a stably stratified fluid. *J. Phys. Oceanogr.* 15:475–77

Winters K, Lombard P, Riley J, D'Asaro E. 1995. Available potential energy and mixing in density-stratified fluids. *J. Fluid Mech.* 289:115–28

Wyngaard JC. 2010. *Turbulence in the Atmosphere.* Cambridge, UK: Cambridge Univ. Press

Yagüe C, Viana S, Maqueda G, Redondo JM. 2006. Influence of stability on the flux-profile relationships for wind speed, ϕ_m, and temperature, ϕ_h, for the stable atmospheric boundary layer. *Nonlinear Proc. Geophys.* 13:185–203

Zhang F, Koch S, Davis C, Kaplan M. 2001. Wavelet analysis and the governing dynamics of a large-amplitude mesoscale gravity-wave event along the East Coast of the United States. *Q. J. R. Meteorol. Soc.* 127:2209–45

Zilitinkevich S, Elperin T, Kleeorin N, Rogachevskii I. 2007. Energy- and flux-budget (EFB) turbulence closure model for stably stratified flows. Part I: steady state homogeneous regimes. *Bound.-Layer Meteorol.* 125:167–91

Zilitinkevich S, Mammarella M, Baklanov AA, Joffre SS. 2008. The effect of stratification on the aerodynamic roughness length and displacement height. *Bound.-Layer Meteorol.* 129:179–90

RELATED RESOURCE

http://www.submeso.org. Visualization of motions in the atmospheric stable boundary layer using networks of data with simulated particles and videos of natural and manmade fog.

Annual Review of
Fluid Mechanics

Volume 46, 2014

Contents

Indexes

Errata

An online log of corrections to *Annual Review of Fluid Mechanics* articles may be found at http://fluid.annualreviews.org/errata.shtml